An Approximate Method to Build an Improved Stress Field in Local Regions

Kee-Nam Song*

(*Received December 2, 1997*)

An approximate procedure to enhance the accuracy of the continuous stress field in local regions has been proposed, based on Loubignac's iterative method and the theory of conjugate approximations. The validity of the proposed method has been tested through three examples: a thick-walled cylinder under internal pressure; an infinite plate with a central circular hole subjected to uniaxial tension; and a short cantilever beam. Analysis of the examples shows that the stress field obtained for the local region model by the proposed method agrees well with that for the whole domain model. In addition, a significant reduction in computing time to obtain the improved stress field implies that the proposed method can be an efficient alternative for the detailed stress analysis in local regions.

Key Words: Displacement-based Finite Element Method, Loubignac's Iterative Method, Conjugate Stress, Projection Method, L_2-norm of Force-imbalance, Total Strain Energy, Local Strain Energy Density, Strain Energy Density Index

1. Introduction

After more than three decades of study and development, the displacement-based finite element method has come to be an effective and widely used tool for numerical analysis in the engineering field because it has following advantages: a simple theory based on the principle of minimizing the total potential energy and a good convergence of the solution. Conventional dis placement-based finite elements maintain only C^0 continuity over the problem domain (Strang and Fix, 1973). In many applications, the quantities of primary interest are not the primary variables, such as displacement and temperature, but rather functions of the derivatives of the primary variables, such as stress and strain, and flux. Since these derivatives do not possess inter-element continuity, a number of post-processing techniques have been developed over the years to interpret these discontinuous fields.

Various methods to overcome these disadvantages have been developed. First, mixed formulations in which the stresses and strains are interpreted independently of the displacements have been used with success in the context of fluid mechanics and visco-elastic flows. However, mixed solution methods have not achieved widespread popularity owing to the large number of solution parameters involved. Second, the projection method, i. e., the theory of conjugate approximations which yields a smooth stress field has been proposed and developed by some researchers (Hinton and Campbell, 1974; Brauchli and Oden, 1971). Even though the stress field from the projection method over the whole domain, such as a global L_2-projection (i. e., least square error method) are continuous over the whole domain, this method requires too much computing time. Therefore, a commercial code, such as ANSYS, employs local L_2-projection over each element and averages the nodal stresses at common nodes to get an improved stress field. Third, Loubignac, Cantin, and Touzot (1977) have proposed an iterative method that improves the accuracy of both stresses and displacements in finite element stress analysis. Then, this method requires too

* Korea Atomic Energy Research Institute, 150 Dukjin-dong, Yuseong-go, Taejon 305-353, Korea

much computation to get an improved stress field and displacement field. In addition, Zienkiewicz, Li, and Nakazawa(1985) proved that the combining of the iterative method with the projection method was consequently identical to the mixed formulation when full convergence was reached. However, the objective of the above methods is to get an improved stress field rather over the entire structure.

In many practical cases, it is necessary to model a small portion of the structure, such as a stress critical component, in greater detail. The first approach to this end is to model the entire structure with a fine mesh. However, this is computationally expensive because large number of equations must be solved. The second approach is to transit from a refined mesh in the area of interest to coarse mesh in the rest of the structure using either triangular elements or specially formulated transition elements. The user may encounter problems generating this type of mesh, especially if a mesh generation preprocessor is being used. The third approach is to solve the problem by subregion modelling, such as the specified displacement method in ANSYS or the zooming method etc. As the stresses by these subregion modelling are also based on the conventional displacement-based finite element analysis, inter-element discontinuities in the stresses still remain.

In this study, an efficient method to build an improved and continuous stress field without further refining the grid in local regions is proposed, based on the theory of conjugate approximations and Loubignac's iterative algorithm. To check the validity of the proposed method, stress analysis on three examples has been carried out.

2. Displacement-based Finite Element Formulation

In the conventional displacement-based finite element method, after a grid is generated over the entire domain, a continuous displacement distribution needs to be assumed for every element (Bathe, 1982). For each element, the displacement field $\{u\}^e$ where superscript e denotes the element, is generally assumed to be:

$$\{u\}^e=[N]\cdot\{\Delta\}^e \tag{1}$$

where $[N]$ is the shape function matrix of the element and $\{\Delta\}^e$ is the displacement vector of the element.

The strain vector $\{\varepsilon\}^e$ can be derived as:

$$\{\varepsilon\}^e=[B]\cdot\{u\}^e \tag{2}$$

where $[B]$ is the element strain matrix.

The stress vector $\{\sigma\}^e$ can be derived as:

$$\{\sigma\}^e=[D]\cdot\{\varepsilon\}^e=[D]\cdot[B]\cdot\{u\}^e \tag{3}$$

where $[D]$ is the constitutive matrix of the material.

The virtual work principle for an element is expressed as:

$$\int_{\Omega e}[B]^T\{\sigma\}^e d\Omega_e=\{F\}^e \tag{4}$$

where Ω_e is the domain of the element, and $\{F\}^e$ is the nodal force vector of the element.

Substituting Eq. (3) into Eq. (4), we have

$$[K]^e=\int_{\Omega e}[B]^T\cdot[D]\cdot[B]d\Omega_e \tag{6}$$

is the stiffness matrix of the element.

3. Conjugate Approximation

Brauchli and Oden(1971) proposed the theory of conjugate approximations and applied the theory for continuous stress field representation in the conforming finite element model. To be brief, the conjugate stress idea is summarized as follows:

1) Consider a finite element model of an elastic body which consists of a collection of E elements connected together at G nodes, and suppose that the finite element model of the displacement components($u_i(x)$) is of the form

$$u_i=\hat{u_i^\triangle}\Phi_\triangle(x) \tag{7}$$

where the repeated index $\triangle$ is summed from 1 to G.

Here $\hat{u_i^\triangle}$ are the components of displacement at node $\triangle$, $i=1, 2, 3$, $\triangle=1, 2, \cdots, G$ and $\Phi_\triangle(x)$ are interpolation functions which have the properties $\Phi_\triangle(x^\Gamma)=\delta_\triangle^\Gamma$; $\triangle, \Gamma=1, 2, \cdots, G$.

2) From the constitutive equations, the conventional stress tensor (σ^{ij}) is obtained from finite element analysis.

$$\sigma^{ij} = E^{ijmn} u_m^{\triangle} \Phi_{\triangle,n}(x) \tag{8}$$

where E^{ijmn} is the elasticity tensor and $\Phi_{\triangle,n}(x) = \frac{\partial \Phi_{\triangle}}{\partial x_n}$, x_n being the material(Cartesian) co-ordinates of x.

3) Conjugate stresses, $S^{ij\triangle}$, and the consistent nodal average, $S_{\triangle}^{ij}$, are defined as follows:

$$S_{\triangle}^{ij} = <\sigma^{ij},\ \Phi_{\triangle}(x)> = \int_{\Omega} \sigma^{ij} \Phi_{\triangle}(x)\, d\Omega \tag{9}$$

$$S^{ij\triangle} = <\sigma^{ij},\ \Phi^{\triangle}(x)> = \int_{\Omega} \sigma^{ij} \Phi^{\triangle}(x)\, d\Omega \tag{10}$$

The conjugated approximation functions, $\Phi^{\triangle}(x)$ are given by

$$\Phi^{\triangle}(x) = C^{\triangle I} \Phi_I(x) \tag{11}$$

Here $C^{\triangle I}$ is the inverse of the matrix $C_{\triangle I}$, defined as follows:

$$C_{\triangle I} S^{ij\triangle} = S_{\triangle}^{ij} \tag{12}$$

where $C_{\triangle I}$ is the fundamental matrix defined as the inner product of the shape functions over the whole domain.

$$C_{\triangle I} = <\Phi_{\triangle}(x),\ \Phi_I(x)> = \int \Phi_I(x) \cdot \Phi_{\triangle}(x)\, d\Omega \tag{13}$$

The major difficulty encountered in applying the theory of consistent stress approximations concerns the matrix $C_{\triangle I}$ of Eq. (12).

4. Stress Improvement in the Local Region

Figure 1 represents the whole domain, which consists of the local region, the outer region, and the interface. The finite element equation for the whole domain can be expressed as follows, where the subscripts 1, 2, and 3 represent the local region, the interface, and the outer region, respectively.

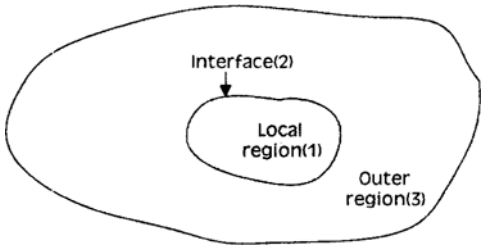

Fig. 1 Illustration of the whole domain and the local region.

$$\begin{bmatrix} K_{11} & K_{12} & 0 \\ K_{21} & K_{22} & K_{23} \\ 0 & K_{32} & K_{33} \end{bmatrix} \begin{pmatrix} u_1 \\ u_2 \\ u_3 \end{pmatrix} = \begin{pmatrix} f_1 \\ f_2 \\ f_3 \end{pmatrix} \tag{14}$$

Discarding the third equation in Eq. (14), the finite element equation, involving only the local region and interface, expressed as subscript L, is as follows:

$$[K]_L u_L = f_L \tag{15}$$

where,

$$[K]_L = \begin{bmatrix} K_{11} & K_{12} \\ K_{21} & K_{22} \end{bmatrix},\ u_L = \begin{pmatrix} u_1 \\ u_2 \end{pmatrix},$$

$$f_L = \begin{pmatrix} f_1 \\ f_2 - K_{23}\ u_3 \end{pmatrix}$$

Jara-Almonte and Knight(1988) showed that by refining the mesh in only the local region and solving Eq. (15), an improved finite element solution could be obtained in the local region. However, in this study, a method to improve the finite element solution in the local region has been proposed by combining the theory of conjugate approximations and Loubignac's iterative method without further refining the grid in the local region(Song, 1997). Applying the conjugate approximation to the whole domain, as in Fig. 1, Eq. (12) can be expressed as follows:

$$\begin{bmatrix} C_{11} & C_{12} & 0 \\ C_{21} & C_{22} & C_{23} \\ 0 & C_{32} & C_{33} \end{bmatrix} \begin{pmatrix} S^1 \\ S^2 \\ S^3 \end{pmatrix} = \begin{pmatrix} S_1 \\ S_2 \\ S_3 \end{pmatrix} \tag{16}$$

where S^i represents the conjugate stress, $S^{ij\triangle}$ defined in Eq. (10) and S_i represents the consistent nodal average, $S_{\triangle}^{ij}$ defined in Eq. (9).

Discarding the third equation in Eq. (16), and supposing that the conventional nodal stress averages (σ_3) in the outer region can replace the conjugate stresses (S^3), Eq. (16) can be approximately reduced as follows:

$$\begin{bmatrix} C_{11} & C_{12} \\ C_{21} & C_{22} \end{bmatrix} \begin{pmatrix} S^1 \\ S^2 \end{pmatrix} = \begin{pmatrix} S_1 \\ S_2 - C_{23} S^3 \end{pmatrix} \approx \begin{pmatrix} S_1 \\ S_2 - C_{23} \sigma_3 \end{pmatrix} \tag{17}$$

Using Eq. (15) and Eq. (17), an improved stress field which is continuous can be obtained iteratively as follows:

i) Solve Eq. (15) to obtain u_L

ii) Calculate the conventional stress field $\sigma_L = [D] \cdot [B] u_L$

iii) Solve Eq. (17) to obtain the conjugate stress S^i

iv) Interpolate the continuous stress field using S^i and the shape function N^*

$$\sigma^* = N_i^* S^i \tag{18}$$

v) Compute the nodal force vector that corresponds to the continuous stress field, σ^*

$$f_e = \int_{\Omega_e} [B]^T \sigma^* d\Omega_e = \int_{\Omega_e} [B]^T N_i^* d\Omega_e \; S^i \tag{19}$$

$$f^* = \sum_{element} f_e = \sum_{element} \int_{\Omega_e} [B]^T \sigma^* d\Omega_e = \sum_{element} \int_{\Omega_e} [B]^T N_i^* d\Omega_e \; S^i \tag{20}$$

The L_2-norm of force-imbalance, $\|\triangle f\|_i$ and the ratio of the L_2-norm of force-imbalance, R_i, at the i-th iteration are defined as follows:

$$\|\triangle f\|_i^2 = \int_{\Omega} (f - f^*)^T \cdot (f - f^*) \, d\Omega$$

$$R_i \equiv \frac{\|\triangle f\|_i}{\|\triangle f\|_0}$$

vi) Solve $\triangle u_L^i = K_L^{-1}(f_L - f^*)$ (21)

vii) Update u_L and σ_L

$$u_L^{i+1} = u_L^i + \triangle u_L^i \tag{22}$$

$$\sigma_L^{i+1} = [D] \cdot [B] u_L^{i+1} \tag{23}$$

viii) Go to step iii) unless $\|\triangle u_L^i\|$ is less than a predefined value.

The total strain energy (U_{total}) expression from the continuous stress field is obtained as:

$$U_{total} = \frac{1}{2} \int_{\Omega} \sigma^{*T} \cdot \varepsilon^* d\Omega = \frac{1}{2} \int_{\Omega} \sigma^{*T} \cdot D^{-1} \cdot \sigma^* d\Omega$$

5. Determination of the Location and Size of the Local Regions

For a given element i, the *local strain energy density*, denoted by $LSED_i$ is defined as:

$$LSED_i = \frac{U_i}{A_i}$$

where U_i and A_i are the strain energy and the area (or volume) in an element i, which are from the conventional finite element solution, respectively.

Similarly, for the whole domain, the *global strain energy density, GSED* is defined as:

$$GSED = \frac{\text{Total strain energy of the system}}{\text{Total volume (or area) of the system}}$$

Many a researcher (Febres-Cedillo and Bhatti, 1988; Botkin and Bennet, 1986; Lee and Lo, 1988) has proposed the strain energy density as an indicator for looking for the location of high-stress concentration or singularities. In this study, the *strain energy density index* ($SEDI$:β_i) for each element is used to discern the location and the size of the local region model.

$$\beta_i \equiv \frac{LSED_i}{GSED}$$

6. Numerical Examples

6.1 Thick-walled cylinder

To show that the present method is effective for smooth problems, a thick-walled cylinder subjected to uniform internal pressure under plane strain conditions is considered. Due to symmetry, one quarter of the cylinder is taken for analysis, as shown in Fig. 2. Poisson's ratio (ν) and Young's modulus (E) are taken to be 0.3 and 1.0, respectively. The finite element model of the problem is shown in Fig. 2 and the shaded region in Fig. 2 represents the local region model discerned by the $SEDI$ whose value is above 1.0. Table 1 represents the value of $SEDI$ in each element layer along radius. The quadrilateral plane strain element has been used in the finite element model. The exact solution (Timoshenko, 1970) is compared with various stress solutions, which come from ANSYS and the present method, over the whole domain and the local region model.

Figures 3 and 4 show the variation of the "ratio of L_2-norm of force imbalance," R_i, as iteration numbers in the whole domain and the local region model, respectively. Figures 3 and 4 show that R_i is monotonously decreasing and rapidly converging in a few iterations. This means that

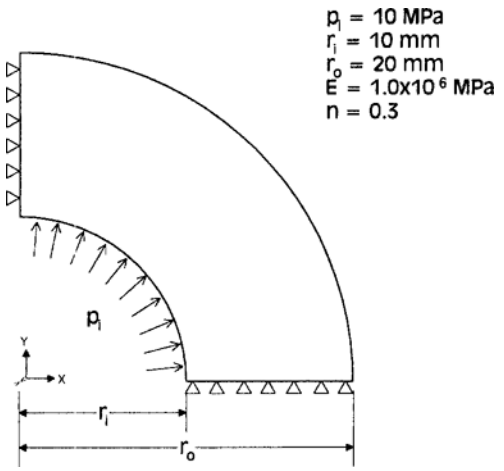

Fig. 2(a) Thick-walled cylinder under internal

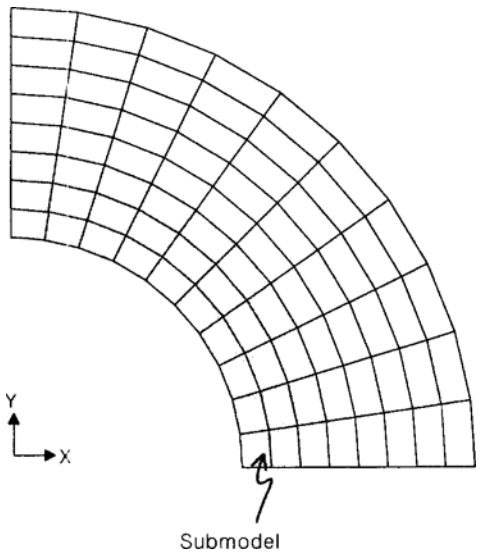

Fig. 2(b) Finite element model of thick-walled cylinder.

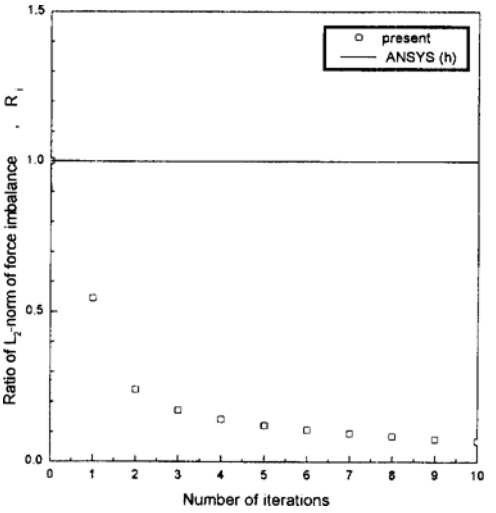

Fig. 3 Ratio of L_2-norm of force imbalance vs. number of iterations in the whole domain.

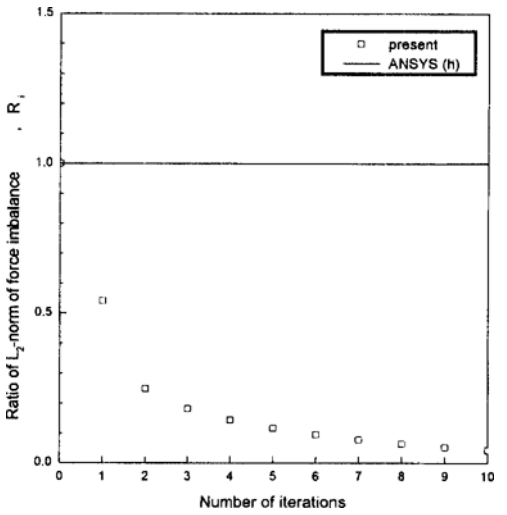

Fig. 4 Ratio of L_2-norm of force imbalance vs. number of iterations in the local region.

Table 1 *SEDI* in the element layer along the radial direction for the thick-walled cylinder.

Element layer from the inner surface	1	2	3	4	5	6	7	8
Strain energy density index (β)	2.937	1.918	1.317	0.945	0.703	0.542	0.430	0.351

the iterative procedure could effectively improve the stress and displacement field, both for the whole domain and the local region model to meet the original finite element equilibrium equation.

Figure 5 shows the comparison of the radial stresses (σ_r) along the inner radius, which are computed iteratively in the local region and the whole domain model from the present study with

the exact solution and the conventional finite element solution (ANSYS results). Three observations are inferred from Fig. 5. First, the nodal stress averages from ANSYS are 21.53% lower than the exact solution for the finite element model of Fig. 2(b), whose maximum node number is 99 and element length is h. In the refined finite element model whose maximum node number is 357 and element length is $\frac{1}{2}h$, the nodal stress averages from ANSYS are 11.31% lower than the exact solution. The stress results from the present study, whether they are from the whole domain model or local region model, are at most 3.47% lower than the exact solution. This shows that the present study can improve the accuracy of the stress figures greatly. Second, the radial stresses (σ_r) from the pure conjugate approximations, i. e., without iteration, are not only 13.6% lower than the exact solution but also 2.3% lower than the nodal stress averages from the refined finite element model. This matches other research (Oden and Reddy, 1973; Brauchli and Oden, 1971) in that conjugate approximations could improve the accuracy of the stress figures. Third, the stress from the local region model is in agreement with that of the whole domain model, except for the presence of a few more oscillations, even though oscillations are also observed in the whole domain model. It seems that the additional oscillations in the local region model are attributed to the assumption that the displacement field (u_3) and stress field (σ_3) in the outer region are fixed, while in fact they may vary at each iteration. In addition, the computing time of the local region model is significantly reduced, compared with that of the whole domain model. Based on the Cyber-960, the computing time for the local region model, whose maximum node number is 33, is 7.076 sec., while that for the whole domain model, whose maximum node number is 99, is

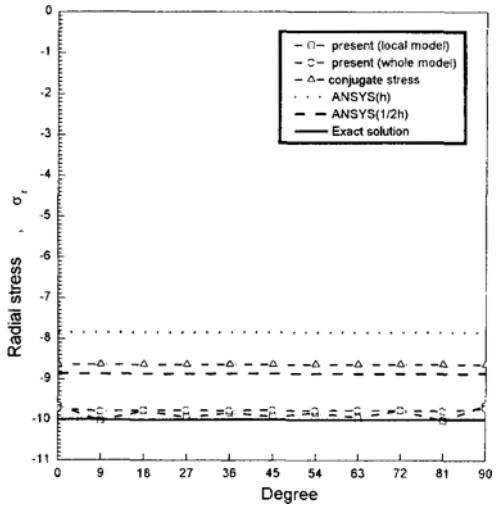

Fig. 5 Variation of the radial stresses along the inner radius.

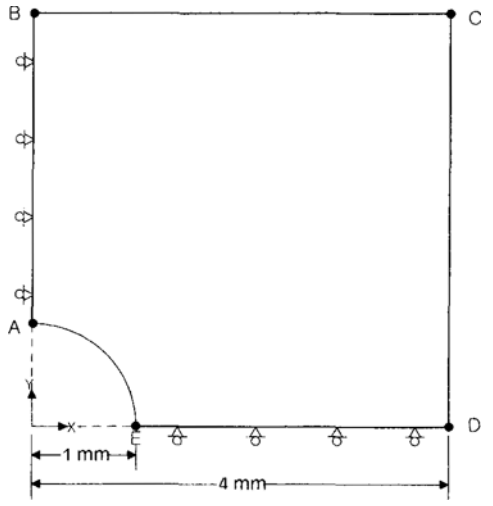

Fig. 6(a) Infinite plate with a central circular hole subjected to unidirectional tension.

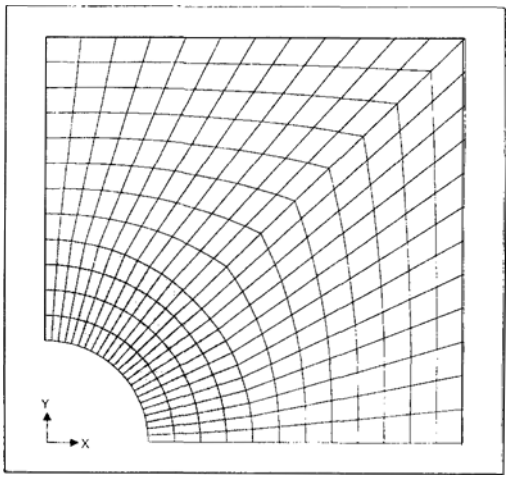

Fig. 6(b) Finite element model of infinite plate with a central circular hole.

316.052 sec. until R_i reaches below 0.1.

6.2 Infinite plate with a central circular hole subjected to uniaxial tensile loads

In the second example, an infinite plate with a central circular hole subjected to a far-field tensile load, $\sigma=1.0$, is considered. Due to symmetry, one-quarter of the cylinder is taken for analysis, as shown in Fig. 6(a). Poisson's ratio and Young's modulus are taken to be 0.3 and 1000, respectively. Plane stress conditions are assumed and boundary conditions are described so that the symmetry conditions are satisfied. The stress boundary conditions(Timoshenko, 1970) are specified along each boundary as follow:

Along BC and CD

$$\sigma_x=1-\frac{a^2}{r^2}\left(\frac{3}{2}\cos 2\theta+\cos 4\theta\right)+\frac{3}{2}\frac{a^4}{r^4}\cos 4\theta$$

$$\sigma_y=-\frac{a^2}{r^2}\left(\frac{1}{2}\cos 2\theta-\cos 4\theta\right)-\frac{3}{2}\frac{a^4}{r^4}\cos 4\theta$$

$$\tau_{xy}=-\frac{a^2}{r^2}\left(\frac{1}{2}\sin 2\theta+\sin 4\theta\right)+\frac{3}{2}\frac{a^4}{r^4}\sin 4\theta$$

$a=1.0$

Along AB and ED

$\tau_{xy}=0$

Along AE

$\sigma_r=0$

$\tau_{r\theta}=0$

Figure 6(b) represents the finite element model with quadrilateral plane stress elements, where the shaded region represents the local region model. Figures 7 and 8 represent the variation of R_i as iteration numbers for the whole domain model whose maximum number is 325 and for the local region model whose maximum number is 125, respectively. Figures 7 and 8 show that R_i significantly decreases and converges in a few iterations. This denotes that the stress fields are being improved to satisfy the original finite element equilibrium equation at a little additional cost of computing time.

Figures (9) ~ (11) represent the variation of σ_r, $\tau_{r\theta}$, and σ_θ along the boundary AE, respectively. Two observations are inferred from Figs. 9 and 10. First, the conjugate stresses are more accurate in approximating the exact solution than the conventional finite element solution. Second, the lack of significant stress differences in the local region model and whole domain model implies that the present study is effective in building an improved and continuous stress field in the local region. Figure 11 shows that there are no significant differences of σ_θ between from the conventional finite element method and the pres-

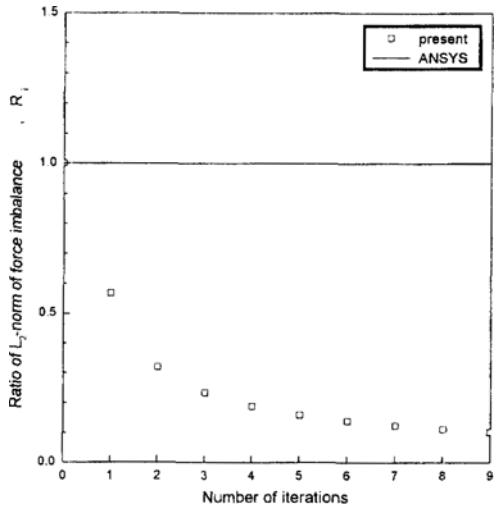

Fig. 7 Ratio of L_2-norm of force imbalance vs. number of iterations in the whole domain.

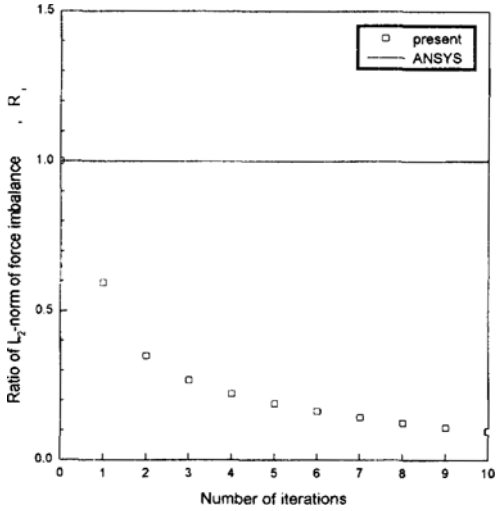

Fig. 8 Ratio of L_2-norm of force imbalance vs. number of iterations in the submodel.

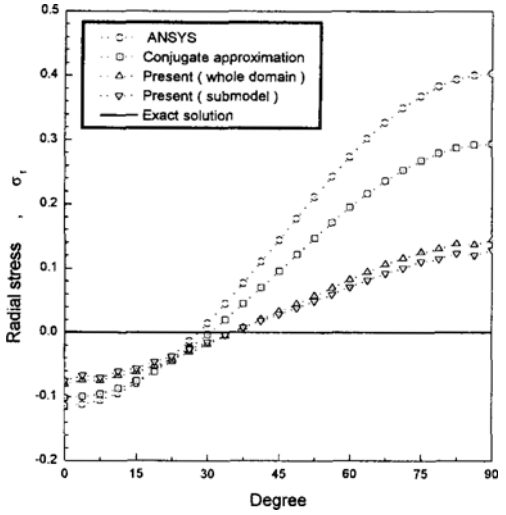

Fig. 9 Variation of the radial stresses along the boundary AE.

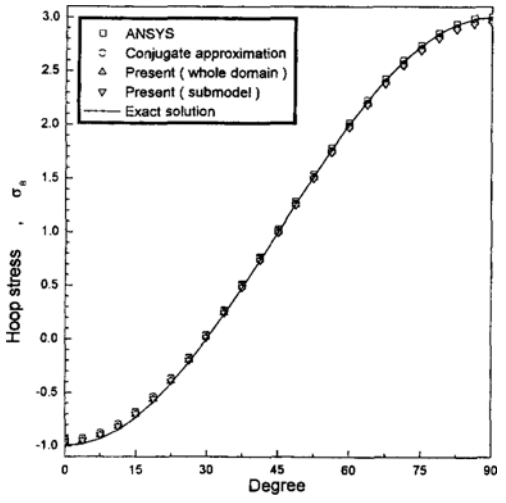

Fig. 11 Variation of the hoop stresses along the boundary AE.

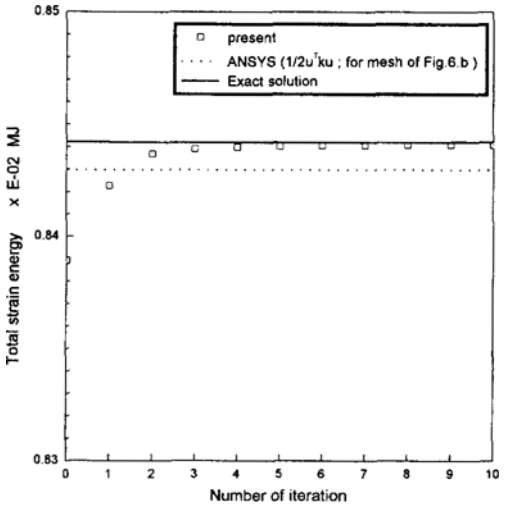

Fig. 10 Variation of the shear stresses along the boundary AE.

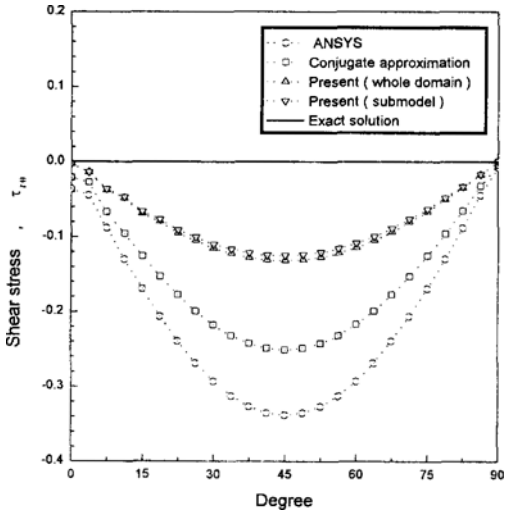

Fig. 12 Total strain energy vs. number of iterations in the whole domain.

ent study.

Figure 12 shows the variation of the total strain energy as iteration numbers increases. The fact that the total strain energy is monotonously increasing as iteration number does and rapidly converging in a few iterations shows that the continuous stress field from this study is continuously being improved to meet the original finite element equilibrium equation.

6.3 Short cantilever beam

A short cantilever beam under plane strain conditions is taken as an example where there are singularities present. The dimensions and the loading and support conditions of the beam are shown in Fig. 13(a). Poisson's ratio and Young's modulus are taken to be 0.3 and 1.0, respectively. Figures 13(b~e) show the various finite element models on quadilateral elements using bilinear basis functions. Total strain energy and R_i at the *5-th* iteration is shown in Table 2.

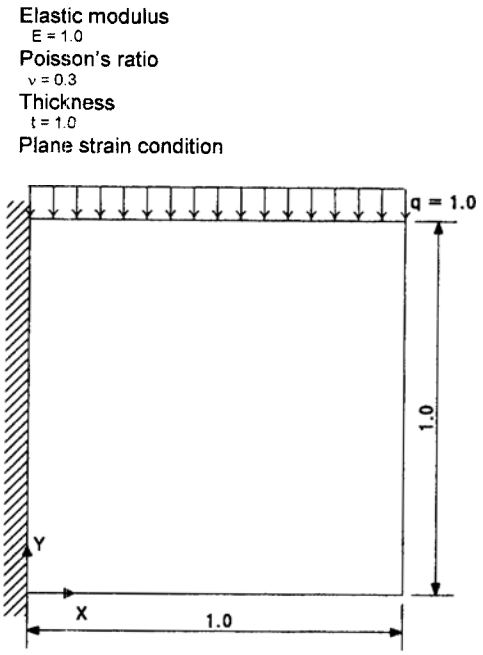

Fig. 13(a) Short cantilever beam

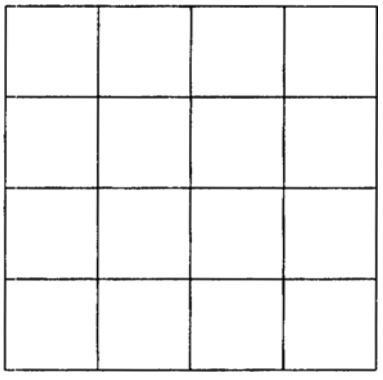

Fig. 13(c) Model 2 (30 DOF)

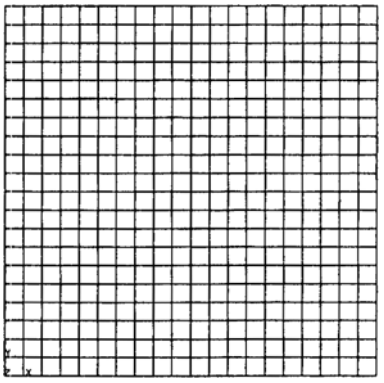

Fig. 13(e) Model 4 (840 DOF)

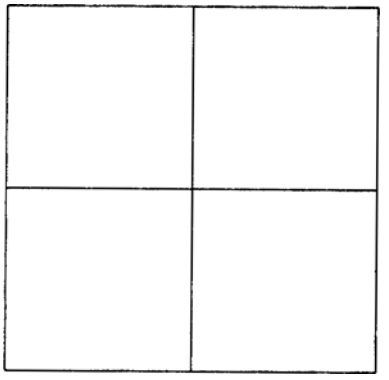

Fig. 13(b) Model 1 (12 DOF)

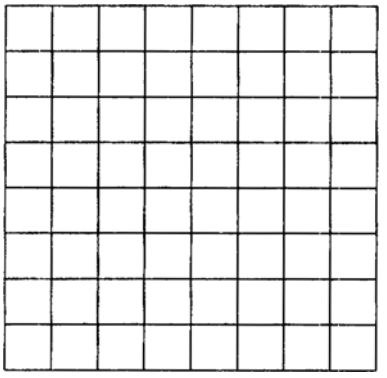

Fig. 13(d) Model 3 (144 DOF)

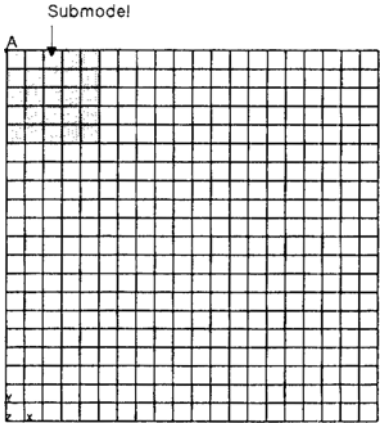

Fig. 13(f) Finite element model.

Table 2 Comparisons of strain energy and R_i for various FE models of the short cantilever beam.

FE Model (DOF)		Total strain energy		R_i
		SE	SE/SE_{exact}	
12	Conventional FEM	0.69511	0.7303	1.000
	Conjugate approximation	0.73866	0.7760	0.47930
	Present study	0.82087	0.8624	0.674E-3
40	Conventional FEM	0.80959	0.8505	1.000
	Conjugate approximation	0.85155	0.8946	0.5725
	Present study	0.90771	0.9536	0.514E-1
144	Conventional FEM	0.88862	0.9336	1.000
	Conjugate approximation	0.91120	0.9573	0.5828
	Present study	0.93613	0.9835	0.1074
840	Conventional GEM	0.93340	0.9806	1.000
	Conjugate approximation	0.94057	0.9881	0.5849
	Present study	0.94769	0.9956	0.927E-1

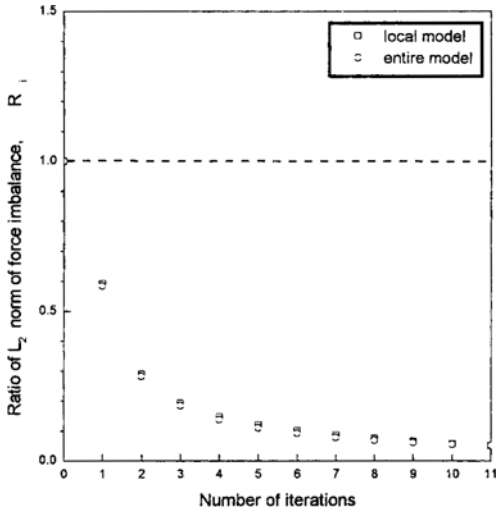

Fig. 14 Ratio of L_2-norm of force imbalance vs. iteration numbers for the short cantilever model.

Table 2 shows that the total strain energy does indeed tend towards the exact value (Ainsworth *et al.*, 1989) as the mesh is refined. Even though the present study employs an iterative method, the present method seems to be a cost effective process since the total strain energy rapidly converges to a certain greater than that of the conventional stress fields in a few iterations.

The shaded region in Fig. 13(f) represents the local region model, which is determined from a conventional finite element solution over the whole domain model. Figure 14 shows the variation of R_i as the iteration number changes for the local region model and whole domain model. Figure 14 shows that R_i is monotonously and rapidly decreasing as the iteration proceeds, which indicates that the stress field is improving to meet the original finite element equations. The maximum normal stress at A in Fig. 13(f) is represented in Table 3, which shows that the maximum stress from the local region model well approximates a value from the whole domain model.

Table 3 Comparisons of maximum normal stress, σ_x at A for the local and whole model.

	Short cantilevers beam	
	Local model	Whole model
Conventional F. E. M.	7.25458	7.25458
Conjugate approximation	7.89336	8.44189
Present study	8.70953	8.74296

7. Conclusions

Combining the theory of conjugate approximations for the stress field and an iterative procedure for the improvement of the displacement field, a

new procedure to build an improved and continuous stress field in the local region has been proposed without further refining the grid. The proposed procedure has been applied to three test examples: two smooth problems and one example where there are singularities. Numerical test results show that the stress fields from the whole domain model and the local region model were both improved to meet the original finite element equilibrium equation and converged in a few iterations. In addition, numerical test results show that not only the stress field from the local region model is seldom different from that of the whole domain model, but also, the computing time to obtain the stress field for the local region model is considerably reduced compared with that for the whole domain model. Therefore, the present method can be used to predict an improved and continuous stress field, both effectively and economically, in the local region where detailed stress analysis is required.

References

Ainsworth, M., Zhu, J. Z., Craig, A. W., and Zienkiewicz, O. C., 1989, "Analysis of the Zienkiewicz-Zhu *a posteriori* Error Estimation in the Finite Element Method," *International Journal for Numerical Methods in Engineering,* Vol. 28, pp. 2161~2174.

ANSYS User's Manual for Revision 5.0, 1992, Swanson Analysis System, Inc.

Bathe, K-J, 1982, *Finite Element Procedure in Engineering Analysis,* Prentice-Hall Inc., Englewood Cliffs, New Jersey.

Botkin, M. E. and Bennet, J. A., 1986, "The Application of Adaptive Mesh Refinement to Shape Optimization of Plate Structures," *in Accuracy Estimates and Adaptive Refinements in Finite Element Computations,* edited by I. Babuska, O. C. Zienkiewicz, J. Gago and E. R. de A. Oliviera), John Wiley & Sons, Chichester, pp. 227~246.

Brauchli, H. J. and Oden, J. T., 1971, "Conjugate Approximation Function in Finite-Element Analysis," *Quarterly of Applied Mathematics,* No. 1, April, pp. 65~90.

Cantin, G., Loubignac, G., and Touzot, G., 1978, "An Iterative Algorithm to Build Continuous Stress and Displacement Solutions," *International Journal for Numerical Methods in Engineering,* Vol. 12, pp. 1492~1506.

Febres-Cedillo, H. E. and Bhatti, M. Asghar, 1988, "A Simple Strain Energy Based Finite Element Mesh Refinement Scheme," *Computers & Structures,* Vol. 28, No. 4, pp. 523~533.

Hinton, E. and Campbell, J. S., 1974, "Local and Global Smoothing of Discontinuous Finite Element Functions Using a Least Squares Method," *International Journal for Numerical Methods in Engineering,* Vol. 8, pp. 461~480.

Jara-Almonte, C. C. and Knight, C. E., 1988, "The Specified Boundary Stiffness/Force SBSF Method for Finite Element Subregion Analysis," *International Journal for Numerical Methods i Engineering,* Vol. 26, pp. 1567~1578.

Lee, C. K. and Lo, S. H., 1988, "An Automat Adaptive Refinement Finite Element Procedu for 2D Elastostatic Analysis," *International Jo nal for Numerical Methods in Engineering,* V 35, pp. 1967~1989.

Loubignac, G., Cantin, G., and Touzot 1977, "Continuous Stress Field in Finite E Analysis," *AIAA Journal,* Vol. 15, No. 1 pp. 1645~1646.

Oden, J. T. and Reddy, J. N., 1973, "N Approximate Method for Computing Conjugate Stresses in Elastic Finite E *International Journal for Numerical Me Engineering,* Vol. 6, pp. 1492~1506.

Song, K. N., 1997, "A Study on the I ment of the Local Stress Field Using the of Conjugate Approximations and Lou Iterative Method," *Transactions of KSM* Vol. 21, No. 10, pp. 1598~1608 (in Kore

Strang, G. and Fix, G. J., 1973, *An Analy the Finite Element Method,* Prentice-Hall Englewood Cliffs, New Jersey.

Timoshenko, S. P., 1970, *Theory of Elasticity,* 3rd ed., McGraw-Hill Kogakusha, Tokyo, pp. 68~71, pp. 90~97.

Zienkiewicz, O. C., Li, Xi-Kui, and Nakazawa S., 1985, "Iterative Solution of Mixed Problems

and the Stress Recovery Procedures," *Communications in Applied Numerical Method,* Vol. 1, pp. 3~9.

Zienkiewicz, O. C. and Zhu, J. Z., 1992, "The Superconvergent Patch Recovery and *a Posteriori* Error Estimates. Part 1: The Recovery Technique," *International Journal for Numerical Methods in Engineering,* Vol. 33, pp. 1331~1364.